RESEARCH MONOGRAPH NO. 8

A numerical model for predicting time-temperature profiles in concrete structures due to the heat of hydration of cementitious materials

Y Ballim

PC Graham
School of Civil and Environmental Engineering,
University of the Witwatersrand

DEPARTMENTS OF CIVIL ENGINEERING
University of Cape Town
University of the Witwatersrand

Published by the Department of Civil Engineering
University of Cape Town

2004

Layout by Tim James
Printed by

Contents

Acknowledgements

The work presented in this monograph draws strongly on the early developmental research undertaken by a number of contributors to our research programme. In particular, the names of Prof. GJ Gibbon, Mr A Benn and Mr P Mokonyama should be mentioned for their contributions to the experimental developments of the research work. The financial contributions of the NRF, THRIP, The Cement Industry through the Cement & Concrete Institute, Eskom and LTA Construction are also gratefully acknowledged

Introduction

When cement is mixed with water, a complex exothermic reaction immediately ensues (Roy, 1989). The heat from this reaction is commonly known as the 'heat of hydration' and it raises the temperature of all the materials in the concrete mixture.

In slender concrete structures with moderate cement contents, the heat of hydration is usually of little consequence because all points in the concrete are close to the surface and the heat generated is rapidly dissipated through the surfaces. However in large concrete structures, where the heart of the concrete is more than approximately one metre from a surface, or in structures with high cement contents (such as a high-strength beam or column), quasi-adiabatic conditions prevail (Taylor and Addis, 1994; Carlson and Forbrich, 1938) and the temperature differential caused by the heat of hydration is the predominant factor contributing to the potential for early age cracking in concrete structures.

The form of variation in thermally induced stress at typical surface and internal points in the concrete is illustrated in Figure 1. During the early stages, when the internal temperature of the immature concrete is increasing, the cooler surface zone (point A) is subjected to tensile stresses and surface cracks, usually fairly shallow, occur within a few days after casting. At later ages, after the peak temperature has been reached and the internal concrete enters the cooling phase, the increased stiffness of the surface zone now acts as a restraint to the thermal shrinkage of the internal concrete. Internal sections (point B) are therefore subjected to tensile stresses and significant internal cracking is possible during this

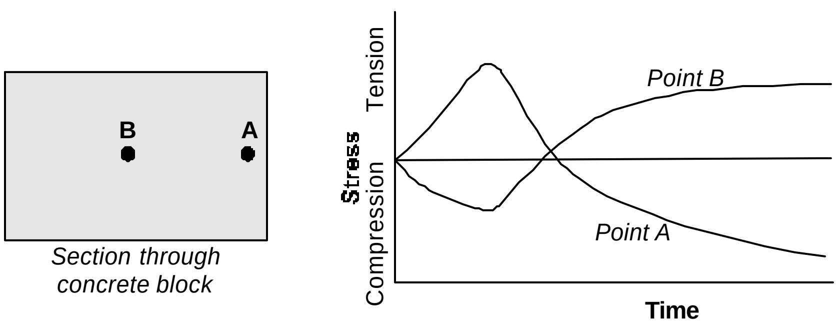

Figure 1: Illustration of the variation of stress at two points in an internal section of a mass concrete element

period (Andersen, 1998). During this phase, the surface sections experience compressive stress.

The purpose of this monograph is to provide designers of concrete structures with a basic numerical model for predicting time-temperature profiles in concrete elements during the early stages of hydration of the cementitious materials. The model is intended as a preliminary design tool and can be used to:

- Provide an early assessment of the likely temperature profiles and gradients in the structure as well as the time-based variations of these profiles;
- Select suitable binder type and binder content for the concrete to be used on the project
- Assess the impact of construction strategies such as artificial cooling of concrete constituents or placing concrete in different seasons, on the likely temperature profiles in the structure.

The model is based on a finite difference numerical solution of the Fourier heat-flow equation and runs in a commercial spreadsheet (Ballim, 2004). Information on the rate of heat evolution of the cementitious binder in the concrete is obtained from laboratory-based adiabatic calorimeter tests (Gibbon et al, 1997). The model uses this information as input and typical heat rate curves for South African cementitious materials are included in the model.

The development of stresses in the concrete and the potential for cracking are based on a complex interaction of temperature gradients, tensile strength, elastic modulus as well as creep and shrinkage capacity. All of these parameters change with time during the early stages of hydration and it is beyond the scope of this monograph to deal with early-age stress development in a complete manner.

The development of the model, its operation and limitations are covered in the text of this monograph. The actual finite difference model, which runs as a Microsoft Excel® file is contained in the compact disk included with this monograph.

Development of the finite-difference temperature model

The flow of heat in concrete is governed by the Fourier equation, which in its two dimensional form is given as:

$$\rho \cdot C_p \cdot \frac{\partial T}{\partial t} = k\left(\frac{\partial^2 T}{\partial x^2} + \frac{\partial^2 T}{\partial y^2}\right) + \frac{\partial q}{\partial t} \qquad (1)$$

where:

?? = density of the concrete
C_p = the specific heat capacity of the concrete
T = temperature
t = time
k = thermal conductivity of the concrete
x, y = the coordinates at a particular point in a structure
q = the heat evolved by the hydrating cement
$\frac{\partial q}{\partial t}$ = is the time rate of heat evolution at point (x, y) in the structure.

Equation 1 is the transient form of the Fourier equation in that temperature at any point in the structure varies with time in first order form, as well as with position (***x; y***) in second order form. Also, the rate of heat evolution is required as input in the solution of Equation 1 and this term is time-dependent because the rate of hydration varies with time. Developing an appropriate form of the rate of heat evolution in concrete is discussed in more detail later.

The temperature prediction model presented in this monograph uses a finite difference numerical technique to solve Equation 1 for a rectangular block of concrete, which has a ***z*** dimension significantly longer than the ***x*** and ***y*** dimensions. As shown in Figure 2, the block is cast onto a rock foundation (thermal conductivity = k_R) and the ambient air temperature (TA) varies with time.

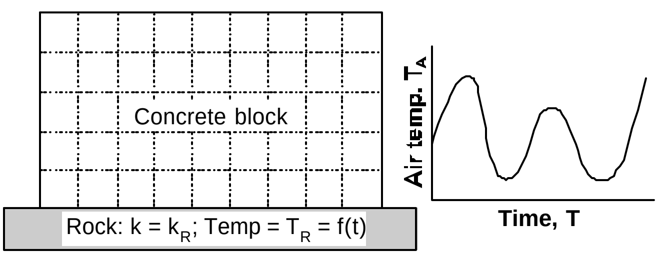

Figure 2: Schematic arrangement of the modelled concrete block.

Developing the node equations

The numerical solution of Equation 1 is covered in a number of texts (Holman, 1990; Dusinberre, 1961; Croft and Lilley, 1977) and only the final form of the finite difference equations for the different situations in the concrete block and associated boundary conditions are presented here. Figure 3 shows the different node positions for which the finite difference equations were developed.

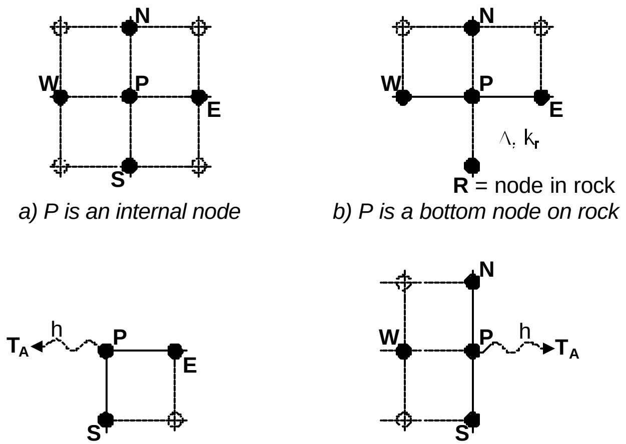

a) *P is an internal node* b) *P is a bottom node on rock*

c) *P is a corner node* d) *P is an exposed edge node*

Note that points N, W, E and S are node points which are adjacent to (and exchange heat with) the point under consideration (point P)

Figure 3: Node positions and boundaries for the finite difference equations

The finite difference equations for each of the conditions shown in Figure 3 are presented below.

Internal nodes (refer to Figure 3a)

$$T_P^{n+1} = \frac{\partial q}{\partial t} \cdot \frac{\delta t}{\rho \cdot C_p} T_P^n (1 - 4 \cdot F_0) + F_0 \left(T_N^n + T_S^n + T_E^n + T_W^n \right) \qquad (2)$$

Subject to:

$$\delta t \le \frac{\rho \cdot C_p \cdot \Delta^2}{4 \cdot k} \qquad (3)$$

where, (in addition to the parameters defined previously):

*   = the temperature at node x in the ith time interval

?***t***   = the time step interval used in the finite difference analysis

C_p = the specific heat capacity of the concrete, determined as the mass weighted average of the individual specific heat capacity of each component in the mix

F_0 = the Fourier Number which is defined as:

$$F_0 = \frac{k \cdot \delta t}{\rho \cdot C_p \Delta^2} \tag{4}$$

? = ?$_x$ = ?$_y$ is the distance between nodes

The limitation on ?t in Equation 3 is to ensure stability of the finite difference model.

Bottom surface nodes (refer to Figure 3b)

A fictitious node, R, is included in the system at a distance * from P and the thermal conductivity of the rock is k_r. The governing equation is then of the form:

$$T_P^{n+1} = \frac{\partial q}{\partial t} \cdot \frac{\delta t}{\rho \cdot C_p} + T_P^n\left[1 - F_0\left(4 + 2\frac{k_r}{k}\right)\right] + F_0\left(2 \cdot T_N^n + T_E^n + T_W^n + 2 \cdot \frac{k_r}{k} \cdot T_R^n\right) \tag{5}$$

subject to:

$$\delta t \leq \frac{\rho \cdot C_p \cdot \Delta^2}{k\left(4 + 2 \cdot \frac{k_r}{k}\right)} \tag{6}$$

The temperature of the rock at node ***R***, * , is taken as the minimum temperature occurring on the previous day. Also, the thermal conductivity of the rock, k_r, is taken as 1.2 W/m.ºC. Where this is critical, the actual thermal conductivity of the base material should be more carefully determined and the model can be adjusted accordingly.

Corner nodes (refer to Figure 3c)

In this case, the heat is also transferred between node P and the environment by convection and the rate of such transfer is determined by the heat transfer coefficient h. The governing equation is then of the form:

$$T_P^{n+1} = \frac{\partial q}{\partial t} \cdot \frac{\delta t}{\rho \cdot C_p} + T_P^n\left[1 - 4 \cdot F_0\left(1 + B_i\right)\right] + 2 \cdot F_0\left(T_E^n + T_S^n + 2 \cdot B_i \cdot T_A^n\right) \tag{7}$$

subject to:

$$\delta t \le \frac{\rho \cdot C_p \cdot \Delta^2}{4 \cdot k(1 + B_i)} \tag{8}$$

where B_i is the Biot number and is defined as:

$$B_i = \frac{h \cdot \Delta}{k} \tag{9}$$

Exposed surface nodes (refer to Figure 3d)

As for the corner nodes, heat is transferred to the environment and the finite difference equation is:

$$T_P^{n+1} = \frac{\partial q}{\partial t} \cdot \frac{\delta t}{\rho \cdot C_p} + T_P^n\left[1 - 4 \cdot F_0\left(1 + \frac{1}{2}B_i\right)\right] + F_0\left(2 \cdot T_W^n + T_N^n + T_S^n + 2 \cdot B_i \cdot T_A^n\right) \tag{10}$$

subject to:

$$\delta t \le \frac{\rho \cdot C_p \cdot \Delta^2}{4(k + h \cdot \Delta)} \tag{11}$$

Modelling the environmental temperature T_A

At the design stage of a construction project, it is unlikely that reliable ambient temperature data are available for the area in which the construction is to take place. This is particularly true when temperature values are required at approximately 1 hour intervals. However, daily ambient maximum and minimum temperatures are usually easily available from the local meteorological office. A model was developed to estimate the ambient temperature at any time, using only the daily maximum and minimum values. This model takes the form:

$$T_A = -\sin\left(\frac{2\pi(t_d + t_m)}{24}\right) \cdot \left(\frac{T_{max} - T_{min}}{2}\right) + \left(\frac{T_{max} + T_{min}}{2}\right) \tag{12}$$

where:

- t_d = the clock time of day at which the prediction is being made (0 to 24 hours)
- t_m = the time at which the minimum overnight temperature occurs (usually at sunrise)
- T_{max} = the maximum temperature for the day under consideration
- T_{min} = the minimum temperature for the day under consideration

The model is fairly rough in that it ignores factors such as cloud cover, wind or direct sunlight and there is probably room for significant refinement. Nevertheless, Figure 4 shows that the model gives a reasonably good prediction when compared with actual measured outdoor temperatures over a period of approximately 10 days.

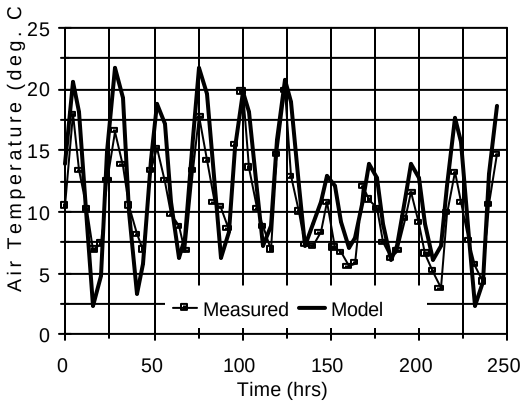

Figure 4: Measured air temperatures compared with the modelled values using Equation 12

Determining the rate of heat evolution of the cementitious binder

The heat of hydration of cement can be determined by means of a test in an adiabatic calorimeter, such as the one described by Gibbon et al (1997) and illustrated schematically in Figure 5. Adiabatic testing is convenient, reproducible and practical. It has the added advantage that the test can be conducted on a sample of the actual concrete to be used in the structure.

In principle the test involves placing a 1litre sample of concrete, immediately after casting, in a water bath, such that a stationary pocket of air separates the sample from the water. The signal from a temperature probe placed in the sample is monitored via an analogue to digital conversion card by a personal computer which switches a heater in the water bath on and off to maintain the water at the same temperature as the concrete sample. This ensures that there is no exchange of heat between the concrete sample and the surrounding environment. The pocket of air around the sample is important because it dampens any harmonic responses between the sample and the water temperatures as a result of the measurement sensitivity of the thermal probes. The test is usually run over a period of 7 days, by which time the rate of heat evolution is too low to be detected as a temperature difference by the thermal probes.

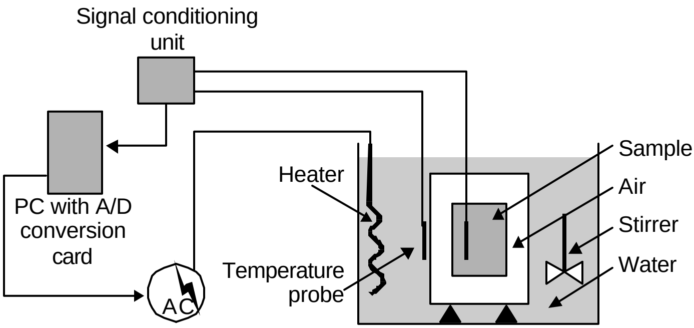

Figure 5: Schematic arrangement of an adiabatic calorimeter

The test produces a curve of temperature vs. time for a particular binder type and mix composition. The total heat evolved at any time by a unit mass of cementitious binder can be determined from the relationship:

$$q = C_p \cdot \delta T \frac{m_s}{m_c} \quad (13)$$

where:

C_p = the specific heat capacity of the sample, is the change in temperature of the sample over the time period under consideration

m_s = the mass of the sample

m_c = the mass of cementitious material in the sample.

The rate of heat evolution can then be determined by means of numerical differentiation with respect to time (t) of the total heat curve, i.e.:

$$\frac{\partial q}{\partial t} \approx \frac{\delta q}{\delta t} \quad (14)$$

An example of the total heat and heat rate curve for a ‘typical’ South African cement, as measured in the Wits University adiabatic calorimeter, is shown in Figure 6.

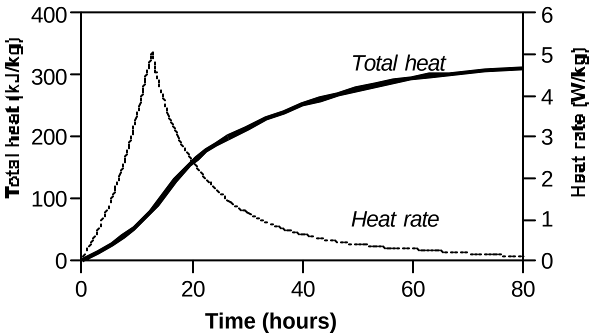

Figure 6: Typical heat curves for a local Portland cement

However, the form of the heat rate relationship shown in Figure 6 is not appropriate for use in solving the Fourier equation (Equation 1). This is because, as a chemical reaction, the rate of hydration of cement is also temperature dependent. The heat rate curve shown in Figure 6 therefore only applies to the unique temperature conditions under which the adiabatic test was conducted. Since different points in a concrete structure can be expected to experience different time-temperature histories, the rate of heat evolution will vary at different points in the structure. To address this problem, Ballim and Graham (2003) describe an approach in which the heat rate is expressed in maturity (or extent of hydration) form, rather than in clock-time form. The approach they proposes uses the Arrhenius form of maturity, which can be written as (based on Naik 1985):

$$M = \sum_{i=1}^{t=n} \exp\left[\left(\frac{E}{R}\right)\left(\frac{1}{293} - \frac{1}{273 + 0.5 \cdot (T_i - T_{i-1})}\right)\right] \cdot (t_i - t_{i-1}) \qquad (15)$$

Where:

M = the equivalent maturity time as for a concrete cured at 20ºC, expressed as t_{20} hours (see Figure 7 below)

E = the activation energy parameter (33.5 kJ/mole) which is taken as a constant (Bamford and Tipper, 1969)

R = the universal gas constant (8.314 J/mole)

T_i = the temperature in ºC at the end of the ith time interval

t_i = clock time at the end of the ith interval

The rate of heat evolution curve can therefore be normalised by expression as a maturity rate of heat evolution:

$$\frac{\partial q}{\partial M}$$

This form of the heat rate curve can then be used as input for solution of Equation 1. The time-based heat rate at each point in the structure at a particular time of analysis is determined from the expression:

$$\frac{\partial q}{\partial t} = \frac{\partial q}{\partial M} \cdot \frac{dM}{dt} \qquad (16)$$

Equation 16 shows that, in the solution to Equation 1 for a concrete structure, it is necessary to monitor the development of maturity as well as the rate of change of maturity at each point under analysis in the structure.

Figure 7 shows the heat curves for the Portland cement presented in Figure 6 above, but expressed in maturity form. In this maturity form, the heat rate curve is suitable for use in a numerical solution of Equation 1.

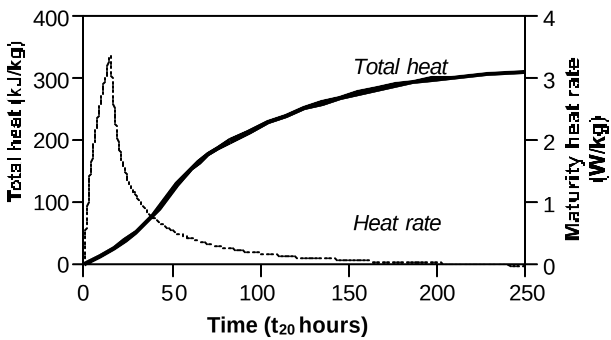

Figure 7: Heat curves of Figure 6 expressed in maturity form.

Graham (2002) showed that the heat-rate profiles of South African cements can vary significantly. Figure 8 shows the range of heat profiles for nine South African cements tested in the adiabatic calorimeter described above.

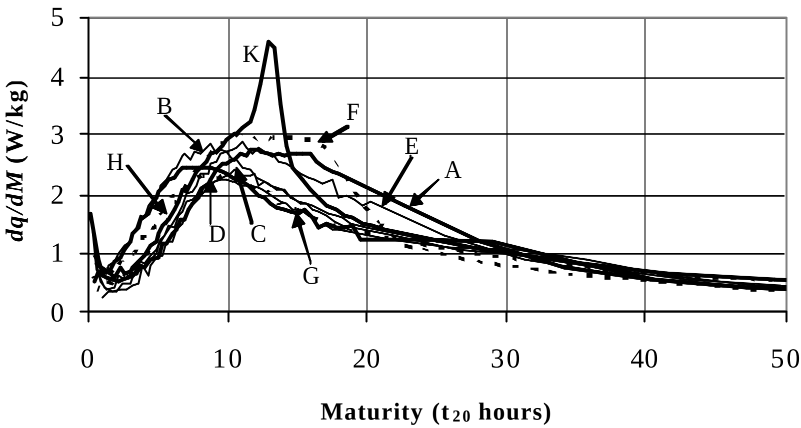

Figure 8: Range of maturity heat-rate profiles for Portland cements drawn from nine production facilities in South Africa (after Graham (2002)).

Operation of the temperature prediction model

Starting up

The temperature prediction model is designed to operate on a desk top computer, using Microsoft Excel 2000® software. The model runs as a macro written in VBA code and the computer should be set up to recognise such macros and alert you to their presence. To the best of our ability, the macro is virus-free and is safe to be enabled. To ensure that the macro can be enabled, proceed as follows:

- open a blank Excel workbook
- select Tools; Macro; Security
- in the 'Security Level' tab, select 'Medium' then 'OK'

The file containing the model can now be opened from the attached compact disc and is titled: ***Ballim Temp Model.xls***. Each modelling exercise must start with a freshly loaded version of this file. When the file is opened, at the security check prompt, select 'enable'.

The file opens on a worksheet titled 'Input' which appears as shown in Figure 9. Click on one of the selection boxes ('Select Binder Type', say). If this shows box-edit markers around the box, rather than a view of the selection menu; do the following:

- deselect the box by clicking on another cell
- select View; Toolbars; Control Toolbox
- in the Control Toolbox, click on the 'Design Mode' icon (the one with a set square, ruler and pencil). This toggles between the 'Edit' and 'Operate' modes of the selection boxes.
- close the Toolbox by clicking on the 'x'

Data should only be entered in the blue areas and selections should be made from the three drop-down menus. There are two other worksheets entitled 'Analysis' and 'Results' which the user should not normally need to access at the model set-up stage. The section below discusses data entry in more detail.

Concrete details section

This section calls for details of the actual concrete being considered for the structure. The mass of the different concrete components should be added in the blue areas. In this case, the admixture content refers to liquid admixtures. The mass of powder chemical admixtures should be added to the sand content.

These quantities are used to calculate the density of the concrete (as the sum of the component masses) and the specific heat capacity of the concrete. The specific heat capacity is taken as the weighted average of the specific heats of the solid materials (taken as 900 J/kg.ºC) and that of the water and liquid admixture (taken as 4190 J/kg.ºC).

Binder type selection

The software allows a selection of one binder type from a list of seven binders. This sets up the measured maturity heat-rate profile for the binder type selected. The selection includes a typical South African CEM I, three blends of this CEM I with ground granulated blast furnace slag (GGBS) and three blends of the CEM I with fly ash (FA). Users wishing to run the model with a different heat-rate profile should contact the authors at the contact details given at the end of this monograph. When a binder type selection is made, the red note on the lower right of the screen will turn off.

Aggregate type selection

The main purpose of this selection is to assign a value of the thermal conductivity of the concrete. Concrete thermal conductivity is strongly influ-

Figure 9: Appearance of the Input worksheet for data entry before running the model

enced by the aggregate type and the software allows a selection from the list of aggregates shown in Table 1. This table also shows the thermal conductivity values that are assigned to the concrete for use in the model. These values have been adapted from those presented by van Breugel (1998).

Table 1: Aggregates types included in the software and corresponding thermal conductivity values.

Aggregate type	*Thermal conductivity (W/m.ºC)*
Quartzite	3.5
Dolomite	3.2
Limestone	3.1
Granite	2.7
Rhyolite	2.2
Basalt	2.1

It should be noted that there can be a range of thermal conductivity values for aggregates which are nominally the same. The values presented in Table 1 are 'average' values and, as with other parameters, are intended to provide a first estimate of the temperatures in the structure.

Again, when an aggregate type selection is made, the red note on the lower right of the screen will turn off.

Construction details section

Concrete casting time

This is the time of day at which the concrete is cast, using a 24-hour clock (e.g. 4.00 pm should be entered as 16). This value is required in using Equation 12 to estimate the ambient temperature at each time interval in the analysis.

Concrete casting temperature

This is the initial temperature of the concrete at the time of casting. This value will appear as the temperature at all nodes in the time t=0 block of the results sheet after the model is run.

The initial temperature of the concrete is an important design and construction variable which can be used to control the temperature profiles in the concrete. Strategies to cool the aggregates or using chilled water as mix water are effective ways to reduce the initial temperature of the concrete. In the absence of a more direct measurement, the initial temperature of the concrete can be estimated from the mass and specific heat weighted average as shown in Equation 17.

$$T_c = \frac{\sum_{i=1}^{n} m_i C_{pi} T_i}{\sum_{i=1}^{n} m_i C_{pi}} \tag{17}$$

where:

T_c = the temperature of the concrete mixture;

m_i = mass of the ith component of the concrete (cement, sand, stone, water, …)

C_{pi} = specific heat capacity of the ith component

T_i = temperature of the ith component at the time it is introduced into the mixer.

The specific heat capacity of the solid materials can be taken as 900 J/kg.^{o}C and that of the water and liquid admixture can be taken as 4190 J/kg.^{o}C.

Formwork type

This is selected from a drop-down menu which has only two selections: timber or steel. This information is necessary to select the appropriate values for the heat transfer coefficient (***h*** in Equations 9 and 11). The model uses a value of 25 W/m^2.^{o}C for all exposed concrete surfaces. This value is appropriate for light wind weather conditions. While the side surfaces are covered with formwork, an ***h*** value of 5 W/m^2.^{o}C is used if the formwork is timber, or 25 W/m^2.^{o}C if steel formwork is used. If no formwork selection is made, the programme defaults to timber formwork. It is assumed that the top surface of the concrete is not covered by any formwork.

Concrete age at formwork removal

As discussed above, this value is used to determine the time at which the value of h should be changed to the exposed value for the side surfaces of the structure.

Maximum and minimum day temperatures

These values are necessary to estimate the ambient temperature at different times during the day using Equation 12. In solving this equation, the model takes tm, the time at which the minimum temperature occurs, as 06h00.

Structure and analysis details section

Horizontal and vertical dimensions of the structure

These are the overall dimensions of the structure and set the limits for the node positions in the model analysis. For a rectangular prismatic structure, the smaller of the two horizontal dimensions should be used as this will represent the direction of steepest temperature gradients.

Space interval (?x = ?y = ?) for analysis

This value determines the spacing of the nodes to be used in the finite-difference analysis. The model temperature predictions will be calculated and reported at each of these nodes. The overall dimension of the structure should be whole number multiples of the space interval selected. If this is not so, the model will extend the overall dimension of the structure to the next nearest node position. There are a few limitations on the value of the space interval selected:

- There should be more than 3 nodes in both directions
- There should be less than 26 nodes in the x direction and less than 39 nodes in the y direction
- For a particular selection of the space interval, the time interval should be small enough to satisfy the conditions set by Equations 3, 6, 8 and 11.

If a value for the space interval is entered and one or more of the conditions mentioned above are not satisfied, an appropriate warning will appear in one of the cells below the ‘Structure and Analysis Details’ box. A different value of space interval should be selected until this warning message is cleared.

Time interval for analysis

This is the ?***t*** used in the model and represents the concrete age intervals at which the analysis is undertaken and temperature results reported. The most important limitation on the time interval is that it should satisfy the conditions set by Equations 3, 6, 8 and 11. If a time interval is selected which does not satisfy all these conditions, an appropriate warning will appear in one of the cells below the ‘Structure and Analysis Details’ box. A smaller value of time interval (or different value of space interval) should be selected until this warning message is cleared. The model does allow factions of an hour to be used and it is good practice to use a time interval of 4 hours or less.

Time duration of analysis

This is the time or concrete age over which the analysis is to be undertaken. The number of time cycles of analysis that will appear in the results sheet is the time duration divided by the time interval selected.

Running the model

After the data fields have been completed in the ‘Input’ worksheet and the appropriate selections have been made, hold down the ‘ctrl’ button and press ‘h’ to run the model. At the end of the model run, the ‘Analysis’ and ‘Input’ worksheets are deleted and the top of the ‘Results’ worksheet is displayed.

The top of the ‘Results’ worksheet shows the basic data that was used in the analysis. Temperature predictions are shown at each node for successively increasing time intervals. Figure 10 shows the first three blocks of results in the analysis of a concrete element measuring 3 m x 2.1 m. The casting temperature of the concrete is 15ºC and the analysis was undertaken in space intervals of 0.3 m with time intervals of 2 hours.

Saving and analysing the results

After the model run, it is important that the results be saved under a new file name using the ‘Save As’ facility. Saving the file without changing the file name may overwrite the master analysis file. Also, the file still contains the macro used for the model analysis but this will no longer operate as a temperature prediction model. It is advisable to delete this macro using the ‘Tools; Macro …’ facility.

The user can now interrogate the data in the ‘Results’ worksheet to consider the time-temperature profiles at different points in the structure. Predicted temperatures at particular points in the structure can also be extracted and compared with temperatures at other points in order to determine the likely temperature gradients in the structure.

SECTION DETAILS			Casting (clock) Time=	11	hrs	k=	3.2	W/m.K	Binder Type=	100% CEM I			
x=	3	m	Start Temp=	15.0	°C	Cp=	1118	J/kg.K	Aggregate Type=	Dolomite	Sand	900	kg/m3
y=	2.1	m	Age at formwork removal=	24	hrs	Density=	2410	kg/m3	Max. day temp=	25 °C	Stone	1100	kg/m3
dx=	0.3	m	11	Nodes in the x direction		Binder Content=	290	kg/m3	Min. day temp=	10 °C	Water	150	kg/m3
dy=	0.3	m	8	Nodes in the y direction		h(min)=	5	W/m2.C	h(max)= 25 W/m2.C	k(rock)= 1.2	Admix	10	kg/m3
Number of time cycles=	100		Time interval=	2	hrs	h=	5						

t=	0.00 hrs										
m	0.00	0.30	0.60	0.90	1.20	1.50	1.80	2.10	2.40	2.70	3.00
0.00	15.0	15.0	15.0	15.0	15.0	15.0	15.0	15.0	15.0	15.0	15.0
0.30	15.0	15.0	15.0	15.0	15.0	15.0	15.0	15.0	15.0	15.0	15.0
0.60	15.0	15.0	15.0	15.0	15.0	15.0	15.0	15.0	15.0	15.0	15.0
0.90	15.0	15.0	15.0	15.0	15.0	15.0	15.0	15.0	15.0	15.0	15.0
1.20	15.0	15.0	15.0	15.0	15.0	15.0	15.0	15.0	15.0	15.0	15.0
1.50	15.0	15.0	15.0	15.0	15.0	15.0	15.0	15.0	15.0	15.0	15.0
1.80	15.0	15.0	15.0	15.0	15.0	15.0	15.0	15.0	15.0	15.0	15.0
2.10	15.0	15.0	15.0	15.0	15.0	15.0	15.0	15.0	15.0	15.0	15.0
t=	2.00 hrs										
m	0.00	0.30	0.60	0.90	1.20	1.50	1.80	2.10	2.40	2.70	3.00
0.00	23.3	19.3	19.3	19.3	19.3	19.3	19.3	19.3	19.3	19.3	23.3
0.30	16.0	15.2	15.2	15.2	15.2	15.2	15.2	15.2	15.2	15.2	16.0
0.60	16.0	15.2	15.2	15.2	15.2	15.2	15.2	15.2	15.2	15.2	16.0
0.90	16.0	15.2	15.2	15.2	15.2	15.2	15.2	15.2	15.2	15.2	16.0
1.20	16.0	15.2	15.2	15.2	15.2	15.2	15.2	15.2	15.2	15.2	16.0
1.50	16.0	15.2	15.2	15.2	15.2	15.2	15.2	15.2	15.2	15.2	16.0
1.80	16.0	15.2	15.2	15.2	15.2	15.2	15.2	15.2	15.2	15.2	16.0
2.10	16.8	15.4	15.4	15.4	15.4	15.4	15.4	15.4	15.4	15.4	16.8
t=	4.00 hrs										
m	0.00	0.30	0.60	0.90	1.20	1.50	1.80	2.10	2.40	2.70	3.00
0.00	23.5	21.9	21.6	21.6	21.6	21.6	21.6	21.6	21.6	21.9	23.5
0.30	17.8	16.2	16.1	16.1	16.1	16.1	16.1	16.1	16.1	16.2	17.8
0.60	17.1	15.8	15.7	15.7	15.7	15.7	15.7	15.7	15.7	15.8	17.1
0.90	17.1	15.8	15.7	15.7	15.7	15.7	15.7	15.7	15.7	15.8	17.1
1.20	17.1	15.8	15.7	15.7	15.7	15.7	15.7	15.7	15.7	15.8	17.1
1.50	17.1	15.8	15.7	15.7	15.7	15.7	15.7	15.7	15.7	15.8	17.1
1.80	17.2	15.8	15.7	15.7	15.7	15.7	15.7	15.7	15.7	15.8	17.2
2.10	18.3	16.1	16.0	16.0	16.0	16.0	16.0	16.0	16.0	16.1	18.3

Figure 10: Example of results for the first three time intervals as produced by the model

Closure

The method described in this monograph provides a simple and reasonably accurate method for predicting temperatures in concrete elements during the early stages of hydration. The model has been structured to be applicable in a wide range of applications. Heat rate data for a typical CEM I and various combinations of FA and GGBS are included in the model.

It must be emphasised that this model was developed as a preliminary design and construction tool and should be used to provide initial estimates of the temperature profiles that are likely to occur in a large concrete element.

The authors welcome any suggestions for improvement of the model or considerations of particular applications for which the parameters included in the model may not be appropriate. We would also appreciate any in situ measurements of concrete temperature which could be used to further verify the model. Please send communications to:

Prof. Yunus Ballim School of Civil & Environmental Egineering
University of the Witwatersrand
Private Bag 3, Wits, 2050, South Africa
Tel: (+2711) 717-7103;
Fax: (+2711) 339-1762
e-mail: ballim@civil.wits.ac.za

Finally, this monograph and the included software are issued without any charge. Please include an appropriate acknowledgement if the results of the model are used in any formal documentation.

References

Andersen, ME (1998). ***Design and construction of concrete structures using temperature and stress calculations to evaluate early-age thermal effects***. In: Materials Science of Concrete V, Skalny, J and Mindess, S (Eds). American Ceramic Society, Westerville, Ohio.

Ballim, Y and Graham, PC (2003). ***A maturity approach to the rate of heat evolution in concrete.*** Magazine of Concrete Research vol. 55, No. 3, pp. 249-256

Ballim, Y (2004). ***Temperature rise in mass concrete elements – Model development and experimental verification using concrete at Katse dam***. Journal of the SAICE, vol. 46, No. 1, pp. 9-14

Bamford, C. H. and Tipper, C. F. H. (eds.) (1969). ***Comprehensive chemical kinetics***, Vol. 1: The practice of kinetics. Elsevier Publishing Company, London.

Carlson, RW and Forbrich, LR (1938). Correlation of methods for measuring heat of hydration. Industrial and Engineering Chemistry (USA), Vol. 10, No. 7, pp: 382-386.

Croft DR and Lilley DG (1977). ***Heat transfer calculations using finite difference equations.*** Applied Science Publishers Ltd., London. 283 pgs.

Dusinberre GM (1961). ***Heat transfer calculations by finite differences.*** International Textbook Company, Pennsylvania, US. 293 pgs.

Gibbon, GJ., Ballim, Y. and Grieve, GRH (1997). ***A low-cost, computer-controlled adiabatic calorimeter for determining the heat of hydration of concrete.*** ASTM Jnl. of Testing and Evaluation, 25, No. 2, pp. 261-266.

Graham, PC (2003). ***The heat evolution characteristics of South African cements and the implications for mass concrete structures.*** PhD Thesis submitted to the University of the Witwatersrand.

Holman, J. P (1990). ***Heat transfer***, 7th Ed. McGraw Hill Inc. New York.

Naik T.R (1985). ***Maturity functions for concrete during winter conditions.*** In: Temperature Effects on Concrete, ASTM STP 858, T.R. Naik, Ed., American Society for Testing and Materials, Philadelphia.

Roy, DM (1989). ***Fly ash and silica fume chemistry and hydration.*** In: Proc. of 3rd International Conference on Fly Ash, Silica Fume, Slag and Natural Pozzolans in concrete. Malhotra, VM (Ed). ACI SP-114. American Concrete Institute, Detroit.

Taylor, PC and Addis, BJ (1994). ***Concrete at early ages.*** In: Fulton’s Concrete Technology, 7th Edition, Portland Cement Institute, Midrand, South Africa.

van Breugel, K (1998). ***Prediction of temperature development in hardening concrete.*** In Prevention of Thermal Cracking in Concrete at Early Ages. Springenschmid, R (ed.), Rilem Report 15. Chapter 4. E&FN Spon, London, pp. 51-75.